International Journal of Photochemistry and Photobiology
2021; 5(2): 28-35
http://www.sciencepublishinggroup.com/j/ijpp
doi: 10.11648/j.ijpp.20210502.13
ISSN: 2640-4281 (Print); ISSN: 2640-429X (Online)

Effect of Increasing Temperature on 1.5 µm Spectroscopic Emission of Er^{3+} Ions Activated Phospho-silicate Thin Film

Eman Helmy Ahmed[1], Magdy Mohamed Hussein Ayoub[1], Ahmed Ismael Hashem[2], Claudia Wickleder[3], Matthias Adlung[3], Amal Amin[1], Inas Kamal Battisha[4, *]

[1]Polymers and Pigments Department, Chemical Industries Research Institute, National Research Centre (NRC), Giza, Egypt

[2]Chemistry Department, Ain Shams University, Cairo, Egypt

[3]Inorganic Chemistry, Faculty of Science and Technology, University of Siegen, Siegen, Germany

[4]Solid State Physics Department, Physics Research Institute, National Research Centre (NRC), Giza, Egypt

Email address:

szbasha@yahoo.com (I. K. Battisha), szbasha5@yahoo.com (I. K. Battisha), ibattisha@gmail.com (I. K. Battisha)

[*]Corresponding author

To cite this article:

Eman Helmy Ahmed, Magdy Mohamed Hussein Ayoub, Ahmed Ismael Hashem, Claudia Wickleder, Matthias Adlung, Amal Amin, Inas Kamal Battisha. Effect of Increasing Temperature on 1.5 µm Spectroscopic Emission of Er^{3+} Ions Activated Phospho-silicate Thin Film. *International Journal of Photochemistry and Photobiology*. Vol. 5, No. 2, 2021, pp. 28-35. doi: 10.11648/j.ijpp.20210502.13

Received: October 16, 2021; **Accepted**: November 15, 2021; **Published**: November 24, 2021

Abstract: Different concentrations of Er^{3+} ions- embedded nano-composite phospho-silicate ranging from 1 up to 3.5 mol % in thin film, symbolic as (S20P), (S20P1Er)T, (S20P2.5Er)T and (S20P3.5Er)T, respectively were prepared as advanced materials for planar waveguide application. Spin coating sol gel technique will be used to prepare the thin films. The prepared thin films optical and spectroscopic assessments were performed using transmittance, absorption, Raman, photoluminescence and refractive index (n) calculations. The observed transmittance T (%) and reflectance R (%) spectra were measured using Jasco V-570 spectrophotometer, in wavelength range (0.2-2.5 µm), confirmed good transparency for the prepared films, where the T (%) was higher than 92% and S20P1ErT was the most transparent one. The mentioned higher transparency presence was considered as a big challenge, especially after doping the silica gel with such higher phosphorus molar percent up to 20 mol %. Such challenge confirmed that the prepared thin films were suitable for the low losses and active planar waveguide fabrication. The room temperature photoluminescence (RTPL) quenching was observed at lower temperature 100°C for (S20P3.5Er)T. Emission at 1.5 µm upon excitation at 514.5 nm was detected and characteristic to the $^4I_{13/2} \rightarrow {}^4I_{15/2}$ erbium ions intra-4F transition for all prepared samples. The morphology of the prepared thin films was examined by using the Field emission scanning electron microscope (FESEM), while the measured film thickness obtained from cross section view from the (FESEM) give rise to 1.791 µm value for (S20P3.5Er)T. The bigger moderate thickness than 1 µm was an adequate parameter for supporting planar optical wave guide applications.

Keywords: Sol-Gel, Thin Film, Photoluminescence, (FESEM), Planar Waveguide

1. Introduction

Sensor devices and data communication are main application fields, which utilize optical waveguides. In data communication applications the transmitted light has been tightly guided inside the waveguide core, which enables to achieve compact device sizes, a tight bending radius and negligible light interaction with the ambient. Enhanced light-ambient interaction is one unique waveguide geometry property, namely slot waveguide, which is the ability to guide and confine the light in high refractive index material embedded between low refractive index materials. Er^{3+} ion has an important emission peak around 1.5 µm corresponding to $^4I_{13/2} \rightarrow {}^4I_{15/2}$ transition. This transition attracted attention due to that it located in the ultra-low-loss telecommunication window of thin film glass, usually observed between around 1400 and 1650 nm wavenumbers. Moreover, Er^{3+} ions exhibited an emission in the green region around 543 nm due to $^4S_{3/2} \rightarrow {}^4I_{15/2}$ intra-4F-Transition [1-3].

Waveguides in rare-earth-doped phospho-silicate have

been fabricated using different methods such as sputtering, sol gel and field-assisted ion exchange methods etc... The used technique in this work is the Sol gel method which is flexible and convenient way to prepare many nano-composite oxide films, powders and monolithic samples as previously reported [4-25]. The spin coating is extensively investigated for optical waveguide fabrication as it produced high quality thin films at room temperature without the need of expensive vacuum systems and standard pressure [12]. Both mesoporous silica and phospho-silicate still remain the more suitable hosts and adsorbents for their unique features such as highly ordered structures and narrow mesopore size distributions [3-5, 10].

The main objective in this work is to report results toward phospho – silicate nano-composites experimental, characterization and theoretical thin film glasses, where they are considered novel modified prepared samples and suitable candidates for planar optical wave guide application. As the most important factor to support planar optical wave guide application is the high enough cross section thickness average values, which is in the present work equal to 1.79 μm for S20P3.5ErT as well as, the film transparency. According to thickness, transparency, refractive indices and luminescence results, it is worthy to mention that S20P3.5ErT was promising to be devised to support planar optical waveguide energy sensor application. Innovative ways to create these waveguides on various substrates were investigated using Er^{3+} ions loaded in phospho-silicate nano-composites S20P with different concentrations to obtain a planar wave guide thin film layered system PWGTFLS. Erbium has special interest in this purpose because it has main emission at wavelength at about 1.54 μm corresponds to fiber optics minimum losses.

2. Materials and Methods

Nano-composites phospho-silicate thin films containing 20 mol % phosphate (SiO_2–20 mol. % P_2O_5) using the tri-ethyl-phosphate as precursor material referred as (S20P). First for the host material silica gel preparation, tetra-ethoxy-silane (TEOS), ethanol (CH_3CH_2OH), distilled water (H_2O) and hydrochloric acid (HCl) were used as precursor materials. The comprised respective molar ratios were 0.028: 0.174: 0.28: 0.0823 for TEOS: CH_3CH_2OH: H_2O: HCl, respectively.

2.1. Thin Films Preparation

Phospho-silicates doped with different Er^{3+} ions concentration were obtained using the mentioned silica molar ratio by hydrolysis and poly-condensation of tetra-ethoxysilane $(CH_3CH_2OH)_4Si$ (TEOS, 99.999%, Sigma-Aldrich) as SiO_2 precursor and Triethyl-phosphate $(C_2H_5O)_3P(O)$ as P_2O_5 precursor in ethanol solution were hydrolyzed under vigorous stirring with distilled H_2O containing HCl used as a catalyst at room temperature for long time. The Er^{3+} ions were introduced in the process, by dissolving Er $(NO_3)_3$-H_2O in distilled water and then to the solution in the preceding precursors mixture with different molar ratios, respectively [20]. Different Er^{3+} ion molars percent were embedded in the prepared S20P film with different Er^{3+} ion concentrations as follow (1, 2.5, and 3.5 mol % Er^{3+}) symbolic as; [S20PEr1T, S20PEr2.5T, andS20PEr3.5T, respectively]. The final used mixture solutions were homogeneous, very clear, and transparent and no precipitates appeared. These solutions were then filtered before performed as thin film.

The obtained homogeneous resultant solutions were used for thin film deposition. The prepared nano-composite solutions were dropped and dispersed on both quartz silica and glass substrates. The solutions then, allowed spinning at 3500 rev. /min for 30 seconds by using a homemade spin coater. At least two successive coatings were required to provide suitable effective film thickness. The film samples were dried for 30 minutes and then heated at different temperature at 500, 700, 800 and 950ºC for 3h, giving cracks free, homogeneous, clear and transparent thin films suitable for planar optical waveguide system PWGTFLS.

2.2. Characterization

Raman was characterized by high sensitive Raman microscope Senterra Bruker laser source 532 nm (Germany) with permanent calibration and high wave number accuracy.

Photoluminescence spectroscopy was performed using 514.5 nm Argon ion laser line as excitation source. The (RTPL) emission and excitation spectra of the presented phospho-silicate nano-composite thin film samples were recorded on Fluorolog spectrofluorometer (HoribaJobinYvon) equipped with Argon laser and a photomultiplier detection system.

Nearly normal transmittance and reflectance spectra were done by Jasco V-570 spectrophotometer, in wavelength range (0.2 -2.5 μm). The refractive indices (n), for all investigated samples were calculated. The refractive index can be expressed in terms of (n) according to the Fresnel equation.

$$n=1 + \sqrt{R} / 1 - \sqrt{R} \quad (1)$$

Nearly normal transmittance and reflectance spectra were done by Jasco V-570 spectrophotometer, in wavelength range (0.2 -2.5 μm).

The morphology of the prepared samples was depicted by using high resolution field emission gun quanta FEG 250 scanning electron microscope (FEHRSEM). The FEHRSEM gives information on the samples surface morphology. The film thickness was measured from FEHRSEM.

3. Results and Discussion

3.1. Raman Microscope

The planar wave guide thin film layer systems PWGTFLS activated by Er^{3+} ions Raman spectra; (a) S20P1ET, (b) S20P2.5ET and (c) S20P3.5ET, respectively, sintered at 950°C for 3h are shown in Figure 1. For higher phosphate concentration at 20 mol % we suggested that the P_2O_5 presence enhances the silica structure modification allowing

the Er^{3+} ions accommodation and solubility with the matrix strain lack. The sol-gel phospho - silicate glass thin films Raman analysis displayed the presence of a very weak and small peak at 233 cm^{-1} in S20PE1T which attributed to the bending vibrations Si-O-P and P-O-P bonding sequences exist in the ternary phospho-silicate system. It was shifted to higher wave numbers at 264 and 266cm^{-1} in [S20PE2.5T and S20PE3.5T] as a result of an increase in Er^{3+} ions concentration as shown in Figure 1. The shoulders at around 390,355 and 336 cm^{-1} were assigned to the P–O–P vibrations in the three prepared thin film samples, respectively. The peaks are not well defined at lower frequencies, as the modes are no longer thought to be localized. However, the strong group peaks between 390and 507 cm^{-1} were assigned to SiO_4 tetrahedron symmetric ring breathing mode involving mainly oxygen motion. It was increased in intensity, broadened and shifted to the higher wave-numbers at higher Er^{3+} ions concentration. The clear change in broadening spectra suggests an Er^{3+} ions wider distribution, where the co-dopant with P_2O_5 has effectively dispersed Er-ions in the glass matrix, avoiding quenching due to Er^{3+} ion pairs or clusters [26, 27]. As the Er^{3+} ions local environment becomes ordered, the inhomogeneous broadening will be limited as typical in the glassy environment due to the elimination of the OH groups at the used higher temperature (950°C) and the non-bridging silicon–oxygen bonds (Si–O–NBO) [26-28].

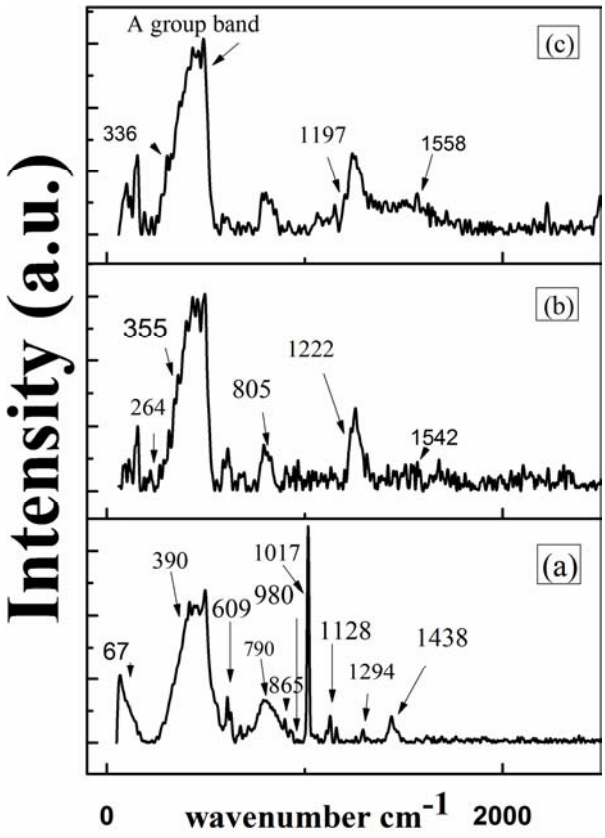

Figure 1. *The PWGTFLS activated by Er^{3+} ions Raman spectra; (a) S20P1ET, (b) S20P2.5ET and (c) S20P3.5ET, respectively, sintered at 950°C for 3h.*

The lower intensity band position and shape changes detected for wave number at 609 cm^{-1} in the prepared samples attributed to the SiO_4 tetrahedral symmetric oxygen breathing vibration of four- and three-member siloxane rings embedded within the glass structure such as the planar rings breathing modes for three- and four-member rings or broken bonds in the vitreous silica network. Phospho-silicate glass is consisting silicon–oxygen, SiO_4, phosphorus– oxygen and $O=PO_3$ tetrahedral bonded randomly in a three-dimensional network, where each silicon atom is bonded with four phosphorus atoms by oxygen linkages. The phosphorus atom has only three such bridging bonds as the regular fourfold and planar three fold ring symmetric stretch signature structures embedded in the more irregular glass network [15].

The broad and weak intense peak at 790 cm^{-1} for S20P1ET broadened and shifted to a higher wave number at about 805 and 810 cm^{-1} at 2.5 and 3.5 mol %, respectively. It is corresponding to Si-O-Si stretching vibration with dominant Si motion; however its broadening might be attributed to the strong intensity of the Si–O–P bands. The very weak and lower intensity peak presence at 865 cm^{-1} corresponding to stretching vibration of non-bridging silicon–oxygen bonds (Si–O–2NBO) might be due to the introduction of phosphate into the silicate network [24]. The asymmetric Si-O-Si stretching apparently appeared as a shoulder at 1222 and 1197 cm^{-1} in S20P2.5ET and S20P3.5ET respectively. A prominent Si-O-NBO stretching was detected at 950-1100 cm^{-1}. A very weak peak near 980 cm^{-1} revealed that the Si-OH stretching was indicating gradual solvent removal at this higher temperature [25]. The 20 mol % P_2O_5 concentration embedded into the random network of SiO_2 tetra-hedra causing several distinct new Raman bands presence.

The sharper and stronger peak at 1017 cm^{-1} in S20P1ET diminished until disappearing at higher Er^{3+} ion concentration, it is corresponding to the PO_3 symmetric stretching vibration. While it is suggested that the small peak at 1128 cm^{-1} might be attributed to P–O–Si (orEr-O) stretching shifted to lower wave-number in both S20P2.5ET and S20P3.5ET, respectively by the Er^{3+}ions addition due to the mixed Si–O–P and/or Si-O-Er linkages vibrations and its intensity decreased by increasing the Er^{3+}ion concentrations, confirming that Er^{3+} ions may have substituted the silica-phosphate lattice site [25]. The Raman band at 1294 cm^{-1} in the S20P1ET was very weak while it became broader and stronger at the higher Er^{3+} ion concentrations. It might be due to the Si-O-P-O-Er presence [26] where the erbium content causes change in both the band position to 1256 and 1241 cm^{-1} and intensities. The weak bands at around 1438, 1542 and 1558cm^{-1} were observed for the three mentioned samples, which are closely matches the frequency of the stretching vibration of O_2 molecules dissolved into the glass structure, which may be corresponds to the tail of the fluorescence band due to the $^4I_{13/2} \rightarrow {}^4I_{15/2}$ transition of the Er^{3+} ions. It might be assigned to a phosphorus centers ($O=PO_3$) tetrahedral stretching vibration surrounded by SiO_4 ones [27-30]. The spectra comparison reveals the presence of high degree of similarity, which suggests that in all these

glasses the main structural units are similar. Nevertheless, certain differences can be noted between the spectra indicated the significant modification of Er^{3+} ions environment in glass systems.

3.2. Optical

Figure 2 a, b and c. shows the PWGTFLS activated by Er^{3+} ions optical transmission (T%) spectra for (a) S20P1ErT, (b) S20P2.5ErT and (c) S20P3.5ErT, respectively, sintered at 950°C. The observed spectra confirmed good transparency for the prepared films, where the T (%) was bigger than 92% in the wavelength ranging from 300 up to 2500 nm and that the S20P1ErT was the most transparent one. The mentioned higher transparency presence was considered a big challenge, especially after doping the silica gel with such higher phosphorus molar percent up to 20 mol %. Such challenge confirmed that the prepared thin films were suitable for the low losses and active planar waveguide fabrication.

Figure 3 shows the PWGTFLS activated by Er^{3+} ions NIR reflectance spectra for (a) S20P1ET (b) S20P2.5 ET and (c) S20P3.5ET, respectively. The obtained data were used in the refractive index calculations using the Fresnel's formula No (1).

The effect of erbium ions concentration on the absorption spectra for the (1, 2.5 & 3.5)T thin film was appeared in Figure 4. It is clearly seen that the absorption peak positions presence were assigned according to the Er^{3+} ions excited levels. The spectrum obtains 10 bands originated from the ground $^4I_{15/2}$ state to different erbium ions excited levels. The peaks at around 343, 385, 406, 446, 485, 522, 660, 800, 963 and 1522 nm were assigned to $^2K_{15/2}$, $^4G_{11/2}$, $^2G_{9/2}$, $^4F_{3/2}$, $^4F_{7/2}$, $^2H_{11/2}$, $^4F_{9/2}$, $^4I_{9/2}$, $^4I_{11/2}$ and $^4I_{13/2}$, respectively. The peaks intensities increased by increasing the Er^{3+} ions concentration. It is important to note that the linear increase in the absorption spectra by increasing the Er^{3+} ions content confirmed the absence of erbium ions chemical clustering. The appeared inset in Figure 4. is an extension of the peak in the area between1500 and 1550 nm for (a) S20P1ET and (b) S20P3.5ET, respectively.

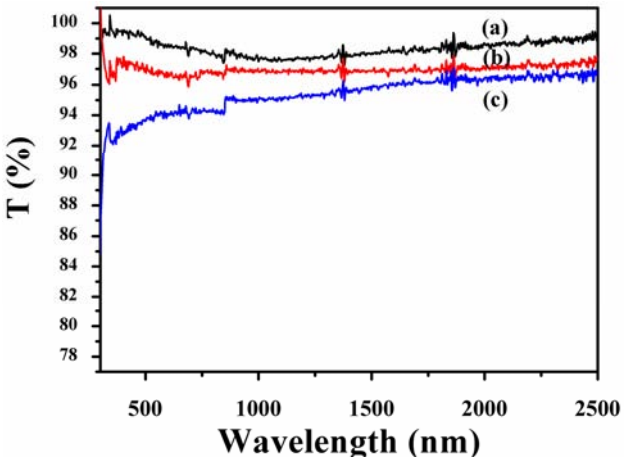

Figure 2. *The PWGTFLS activated by Er^{3+} ions Optical transmission spectrum for (a) S20P1ET, (b) S20P3.5ET & (c) S20P3.5ET, respectively, sintered at 950°C for 3h.*

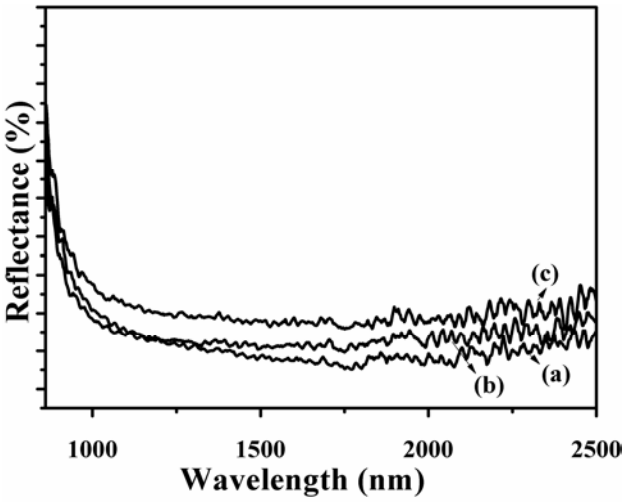

Figure 3. *The PWGTFLS activated by Er^{3+} ions NIR reflectance spectra for (a) S20P1ET (b) S20P2.5 ET and (c) S20P3.5ET, respectively sintered at 950°C for 3h.*

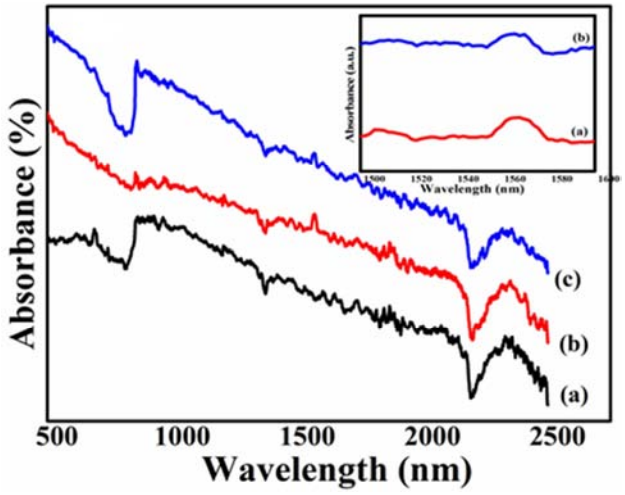

Figure 4. *The PWGTFLS activated by Er^{3+} ions absorption spectra for (a) S20P1ET, (b) S20P3.5ET & (c) S20P3.5ET, respectively, sintered at 950°C for 3h. The inset is the extension for (a) S20P1ET and (b) S20P3.5ET, sintered at 950°C, for focusing on NIR region between 1500 and 1550 nm.*

Figure 5 A & B were drawn to highlight on the refractive index (n) behavior for SPT and the PWGTFLS activated by Er^{3+} ions of S20P1ErT, S20P2.5ErT and S20P3.5ErT, respectively sintered at (A) 500 and (B) 950°C deposited on glass and silica substrates. The refractive indices (n) values were obtained at constant wavelength 1768 nm giving the following values; 1.699, 1.711, 1.730 and 1.745, sintered at 500°C and 1.701, 1.713, 1.7493 and 1.7512 sintered at 950°C, respectively. Table 1 and Figure 5 give information of the increment in the (n) values by increasing both Er^{3+} ion concentrations and sintering temperature, associated with the materials condensation and densification. When the cation modifier phosphate and Er^{3+} ions are present in the silica- gel it causes the Si–O–Si bonds broken and the non-bonding oxygen (NBOs) presence, subsequently increasing the network molar volume structure [31, 32]. Moreover, by increasing both the erbium ion concentrations and the sintering temperature; (n) linearly increased due to the

densification, the change in the chemical structure, the re-arrangement and re-crystallization of the nano-composite phospho-silicate [31, 32].

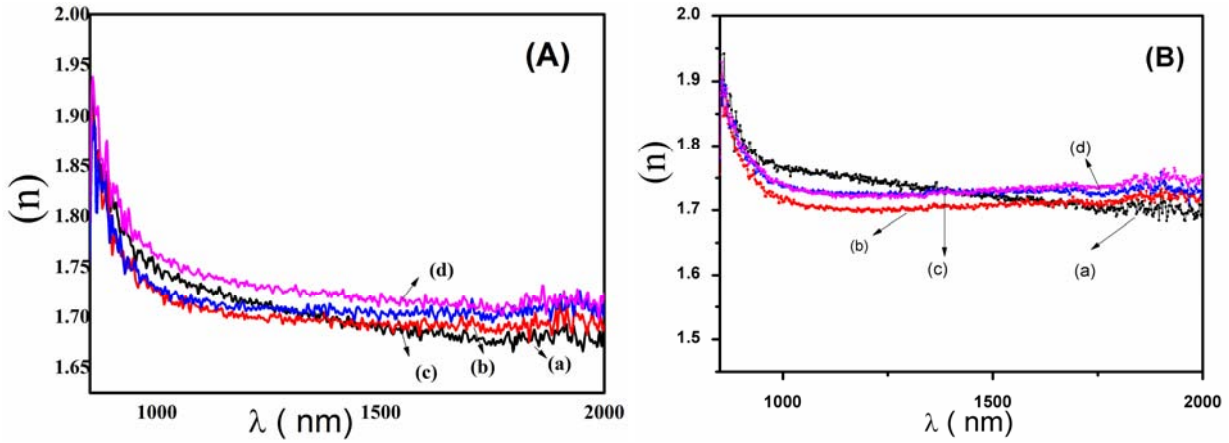

Figure 5. *The PWGTFLS activated by Er^{3+} ions refractive index (n) of (a) S20PT, (b) S20P1ET, (c) S20P2.5ET& (d) S20P3.5ET, (A) sintered at 500°C and (B) at 950°C for 3h.*

3.3. Morphology

Figures 6 & 7 show the PWGTFLS activated by Er^{3+} ions surface morphology micrographs and the cross-section views for (a) S20P1ErT, (b) S20P2.5ErT and (c) S20P3.5ErT, sintered at constant temperature 950°C for 3h. Smooth and homogeneous surfaces were appeared for the three mentioned samples as in Figure 6. On the other side Table 2. summarized the thin film thicknesses measured values using the FEHRSEM cross section views shown in Figure 7. It was observed that the average thin film thickness values were increased by increasing the Er^{3+} ion concentrations from 1.151038 µm at 1 mol. % up to 1.791µm at 3.5 mol %, respectively.

Table 1. *Refractive index (n) for the S20PT and WGTFLS S20P1ET, S20P2.5ET and S20P3.5ET, respectively.*

Sample label	Refractive index (±0.0004)	
	500°C	95°C
S20PT	1.699	1.701
S20P1ET	1.711	1.713
S20P2.5ET	1.73	1.7493
S20P3.5ET	1.745	1.7512

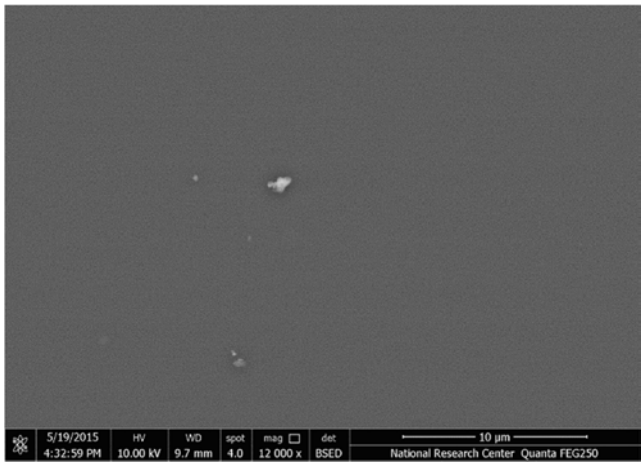

(a)

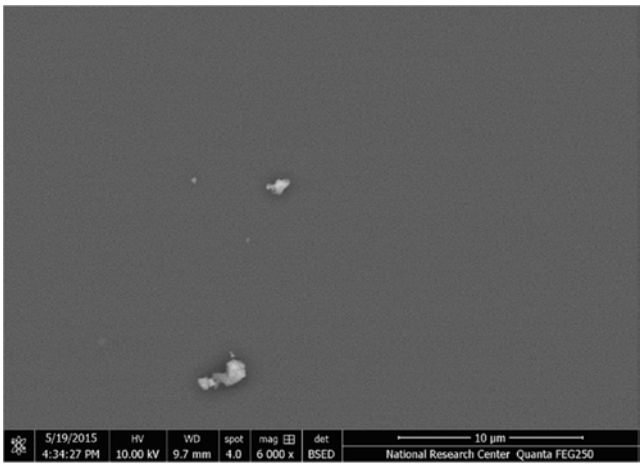

(b)

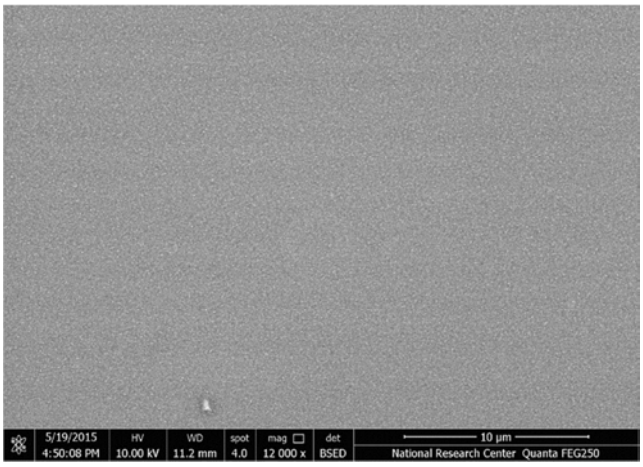

(c)

Figure 6. *a, b and c. The PWGTFLS activated by Er^{3+} ions for the FEHRSEM surface morphology micrographs of (a) S20P1ET, (b) S20P2.5ET & (c) S20P3.5ET, sintered at 500°C for 3h.*

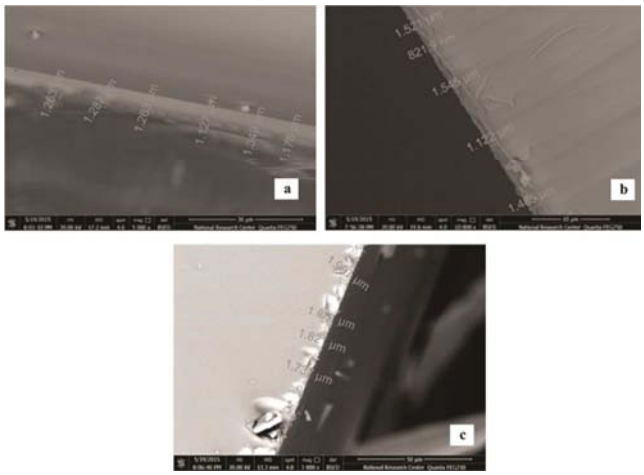

Figure 7. *The PWGTFLS activated by Er^{3+} ions for FESEM cross section figures of (a) SP1ErT, (b) SP2.5ErT & (c) SP3.5ErT, respectively, sintered at 500°C for 3h.*

Table 2. *The thickness values of WGTFLS; S20P1ET, S20P2.5ET and S20P3.5ET, respectively.*

Sample	S20P1ET	S20P2.5ET	S20P3.5ET
Thickness	1.521µm	1.263µm	1.997µm
	821.9nm	1.287µm	1.821µm
	1.545µm	1.263µm	1.609µm
	1.122µm	1.127µm	1.737µm
	1.485µm	1.349µm	
		1.178µm	
Average	1.151038µm	1.2445µm	1.791µm

We can conclude that by increasing the sintering temperature, a transparent (higher than 92%) PWGTFLS S20P (1-3.5) ET will be successfully obtained. The prepared films exhibit higher thickness higher than 1 µm equal to 1.791 and higher refractive index at constant wavelength 1768 nm ranging from 1.701 up to 1.7512 sintered at constant temperature 950°C, illustrating the possibility of PWGTFLS activated by Er^{3+} ions to be successfully prepared and characterized. These obtained data allowed the low loss systems waveguide PWGTFLS application, which was the goal of this work.

3.4. Photoluminescence

The phosphate is an excellent dopant material embedded in silica gel due to its high stimulated emission cross-section, ion exchange ability, high gain coefficient, removing clusters and low up-conversion emission. For these purposes we tried here to study the effect of increasing the sintering temperature from 100 up to 950°C of the representative PWGTFLS activated by Er^{3+} ions of S20P3.5ErT by measuring the (RTPNIR) spectra transition upon excitation with 514.5 nm argon lasers, as drawn in Figure 8. It was observed that by increasing the sintering temperature from 100 up to 950°C, the luminescence from the first excited $^4I_{13/2}$ state of erbium ions was obtained, with a main emission peak at about 1.54 µm. Higher intensity at 950°C was observed which decreased and the peak became broader at lower sintering temperature. A quenching phenomenon was characteristic these spectra at lower temperature, where the samples with lower PL peaks had OH resident groups at this lower temperature. However, the sintered film at lower temperature at 100°C had more residual porosity, indicating that the PL quenching was associated with an increase of OH-related species in incompletely densified porous gel at lower temperature. The obtained data are in compatible with the previously reported by C. Duverger et al., [33] who suggested that the fluorescence decay at the 1.5 µm region was affected by the O-H stretching vibration presence and depended on the densification process and the removal of O-H group at higher sintering temperature. Generally the band flatness increased by increasing the inhomogeneous broadening at lower sintering temperature. When the densification was achieved causing pores to be closed site - to- site in homogeneity.

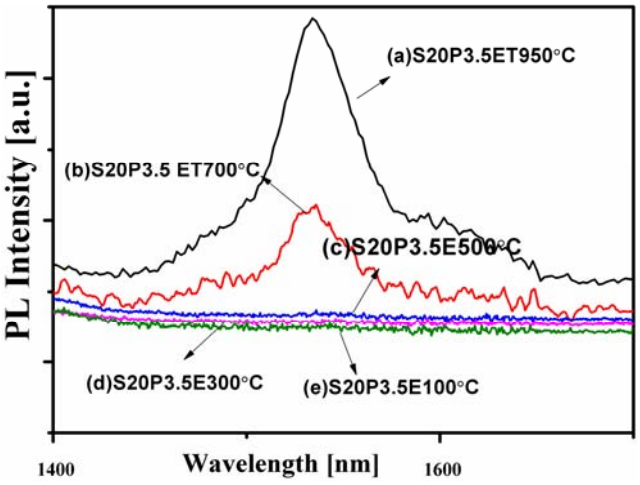

Figure 8. *The PWGTFLS activated by Er^{3+} ions RTPLNIR spectra of Er^{3+} ions after excitation with 514.5 nm for S20P3.5ET sintered from 100 up to 950°C for 3h.*

Figure 9 shows the expected diagram for total internal reflection process (the light propagation) inside the PWGTFLS activated by Er^{3+} ions of S20P1ET, S20P2.5ET and S20P3.5ET prepared samples.

In short, the most important factors to support planar optical wave guide application are the higher cross section values, higher transparency (92%) and higher refractive indices of the prepared films as well as the RTPL results at NIR region between 1.500 and 1.550 µm causing S20P1ErT, S20P2.5ErT and S20P3.5ErT to support PWGTFLS planar optical waveguide thin film layers system application.

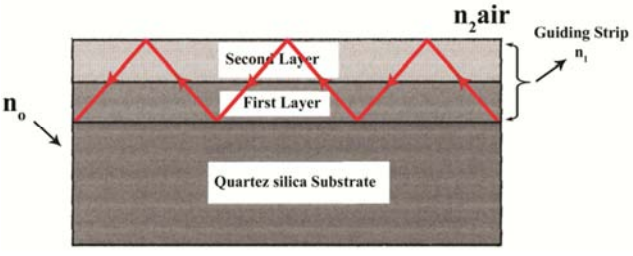

Figure 9. *The expected diagram of the light propagation process inside the S20P1ET, S20P2.5ET & S20P3.5ET, respectively.*

4. Conclusion

Modified sol gel method was successfully used for the preparation of both nano-composites phospho-silicate S20P and the PWGTFLS activated by Er^{3+} ions S20P loaded with (1 up to 3.5) mol % Er^{3+} ions S20P(1-3.5)ET in thin film form. Recorded optical transmissions data reported a brief prove for transparency challenge which reached more than 92% for PWGTFLS fabrication. The phospho - silicate activated by erbium ions was shown to induce increase in the refractive index, transparency and thickness. The S20P thin film doped with different concentrations of Er^{3+} ions at 1, 2.5 and 3.5 mol % refractive indices showed the following values 1.701, 1.713, 1.7493 and 1.7512, respectively, at proper constant annealing temperature 950°C. The prepared materials had an increment in refractive index variation illustrating their successful utilization in PWGTFLS. The bigger moderate thickness than 1 μm was an adequate parameter for planar waveguide thin film layers system applications.

The erbium doped prepared thin film samples emit light in the region between 1.500 up to 1.550 μm up on excitation source at 514.5 nm due to the 4f shell transition from the first excited state $^4I_{13/2}$ to the ground state $^4I_{15/2}$ of it.

Funding

This study was funded by normal fund of National Research Centre NRC for PhD student which is 12000 Egyptian pounds.

Conflict of Interest

Authors; Prof. M. Ayoub, Dr. A. Amin, Prof. I. K. Battisha and the student Eman H Ahmed have received normal fund of National Research Centre for PhD student which is 12000 Egyptian pounds.

Acknowledgements

The authors acknowledge the team work of the Italian – Egyptian sharing project entitled [Smart optical nanostructures for green photonics] especially Prof. Maurizio Ferrari for his great support, 2013 – 2019.

References

[1] Y. Yamada. H. Ono, T. Kanamori, Y. Ohishi. (1997). Broadband and Gain Flattened Amplifier Composed of a 1.55 μm-Band and 1.58 μm-Band Er^{+3} - Doped Fiber Amplifier in a Parallel Configuration. *Elect. Lett.* 33 710-711.

[2] Y. Ohishi, A. Mori, M. Yamada, H. Ono, Y. Nishida, K. Oikawa. (1998). Gain Characteristics of Tellurite-Based Erbium-Doped Fiber Amplifiers for 1.5-μm Broadband Amplification. *J. of Opt. Lett* 23 274-276.

[3] A. Amin, E. H. Ahmed, C. Wickleder, M. Adlung, A. I. Hashem, M. H. Ayoub and I. K. Battisha. (2019). Phosphosilicate–Polyamidoamine Hyperbranched Polymer–Er^{3+} Nanocomposite Toward Planar Optical Waveguide Applications. *J. of Polym. Compos*. 2029 -2038.

[4] H. A. Wahab, A. A. El Saeid, A. A. Salama, I. K. Battisha. (2021) Zinc Oxide nano-rods: challenges for glucose biosensors, Egyptian J. of Chemistry, *Egypt. J. Chem* 64, (3) 1219-1227.

[5] I. K. Battisha, M. M. H. Ayoub, A. I. Hashem, E. H. Ahmed and A. Amin. (2017). Thermal Effect of Er^{3+} Ions Embedded in Smart Nano-composite Oxide Material Prepared by Sol Gel Technique. *J. Acta Physica Polinica A*. 132, 41277-1283.

[6] I. k. Battisha. (2004). Visible Up-Conversion Luminescence in Ho $^{3+}$: $BaTiO_3$ Nano-Crystals Prepared by Sol Gel Technique. *J. Solgel Sci. Technol*. 30 (3) 163–172.

[7] H. A. Wahab, A. A. Salama, A. A. El Saeid and I. K. Battisha (2018) Development of ZN_R- Calcium Biosensors Application. *J. of Advances in natural sciences: Nano-science and Nano-technology*. 9 1-5.

[8] H. A. Wahab, I. K. Battisha, A. A. El Saeid and A. A. Salama (2018). Nano-Rods Oxide Materials for Biosensor Application, Egypt. J. Biophys. Biomed. Engng. 19 45-50.

[9] H. A. Wahab, A. A. Salama, A. A. El Saeid, M. Willander, O. Nur, I. K. Battisha. (2018) Zinc Oxide Nano-Rods Based Glucose Bbiosensor Devices Fabrication, *J. Of Results in Physics*. 9 809-814.

[10] I. K. Battisha. (2002). Structural and Optical Properties of Monolithic Silica Gel Glasses Containing Nd^{3+} Using Two Different Precursors TEOS and TMOS Prepared By Sol-gel. *Indian J. of Pure and Appl. Phys.* 40 122-131.

[11] I. K. Battisha, H. A. Wahab, A. A. Salama, A. A. El Saeid, M. Willander, and O. Nur. (2015). Semiconductor ZnO Nano-rods Thin Film Grown On Silver Wire For Hemoglobin Biosensor Fabrication. *New Journal of Glass and Ceramics (NJGC)* 5: 9-15.

[12] H. H. Mahmouda, I. K. Battisha b, F. M. Ezz-Eldin. (2015). Structural, Optical and Magnetic Properties of Irradiated SiO_2 Xerogel Doped Fe_2O_3. *Spectrochimica Acta Part A: Molecular and Biomolecular Spectroscopy*. 150 72–82.

[13] H. Shaier, A. Salah, W. M. Mousa, S. S. Hamed and I. K. Battisha. (2020). Physical Properties and Up- Conversion Development of Ho^{3+} Ions Loaded Nano-Composite Silica Titania Thin Film, *Journal of Materials research express Mater. Res. Express.* 7 096403.

[14] O. El-sayed, I. K. Battisha, A. lahmar and M. El Marssi. (2021). Er^{3+} and Er^{3+}/Yb^{3+} Ions Embedded in Nano-Structure BaTi0.9Sn0.1O3: Structure, Morphology and Dielectric Properties. *World Journal of Nano Science and Engineering,* 11 25-43.

[15] I. K. Battisha. (2002). Physical Properties of Nano-Particle Silica Gel Doped With CdS Prepared by Sol-Gel Technique. *J. of Fizika A.* 11 34001-34010.

[16] I. K. Battisha, A. Speghini, S. Polizzi, F. Agnoli and M. Bettinelli. (2002). Molten Chloride Synthesis, Structural Characterization and Luminescence Spectroscopy of Ultra-Fine Eu^{3+} Doped $BaTiO_3$ and $SrTiO_3$. *J. of Material Letter.* 57/1: 83-187.

[17] Y. Badr, A. Salah and I. K. Battisha IK. *(2005)*. Effect of Europium Ion Concentrations on The Up-Conversion Emission of Nano-Crystalline $BaTiO_3$ Prepared by Sol-Gel Technique, J. of Sol-gel science and technology, *J SOL-GEL SCI TECHN*. 34 219-226.

[18] Talaat A. Hameed, F. Mohamed, A. M. Mansour, I. K. Battisha. (2019). Synthesis of Sm^{3+} and Gd^{3+} Ions Embedded in Nano-Structure Barium Titanate Pprepared by Sol Gel Technique: Terahertz, Dielectric and Up conversion Study. *J. of ECS Journal of Solid State Science and Technology. ECS J SOLID STATE SC*. 9 123005.

[19] E. H. Ahmed, M. M. H Ayoub, A. I. Hashem, I. K. Battisha, C. Wickleder, M. Adlung, A. Amin. (2021). Nanocomposites Dendritic Polyamidoamine Based Chitosan Hyperbranched Polymer Embedded in Silica – Phosphate for Waveguide Applications. *J. of Polymer-Plastics Technology and Engineering, Polym Plast Technol Eng*. 60 7 744–755.

[20] R. Mahani, O. El-sayed, S. El-Mahy, I. K. Battisha. (2020). Structure and Dielectric Studies of Co-Doped $BaTiO_3$ With Sn^{4+}/ Er^{3+} Ions. *J of Acta Polynica A*. 137 410-416. DOI: 10.12693/APhysPolA.126.1318.

[21] O. El-Sayed, W. M. Mousa, A. Zeinert, A. lahmar, M. El Marssi, I. K. Battisha. (2020). Calcination Temperature Effect on Dielectric, Structural and Morphology Properties of $BaTiO_3$ Nano-Structure Prepared by Modified Sol – Gel Technique. *J. of Adv. Nat. Sci.: Nanosci. Nanotechnol*. 11 015015 (1-8).

[22] A. Salah, S. El-Mahy, O. El-sayed, I. K. Battisha. (2020). Up-conversion Behaviors of Nano-Structure $BaTi_{0.9}Sn_{0.1}O_3$ Activated by Er^{3+}/Yb^{3+} Ions. *Optik - International Journal for Light and Electron Optics*. 209 164571 (1-9).

[23] A. Lukowiak, A. Chiappini, A. Chiasera, D. Ristic, I. Vasilchenko, C. Armellini, A. Carpentiero, S. Varas, G. Speranza, S. Taccheo, S. Pelli, I. K. Battisha, G. C. Righini, W. Strek and M. Ferrari. (2015). Sol–Gel-Derived Photonic Structures Handling Erbium Ions Luminescence. *J. of Opt Quant Electron. Opt Quant Electron*. 47 117-124.

[24] A. Lukowiak, R. J. Wiglusz, A. Chiappini, C. Armellini, I. K. Battisha, G. C. Righini and M. Ferrari. (2014). Structural and Spectroscopic Properties of Eu^{3+}-Activated Nanocrystalline: Tetra-Phosphates Loaded in Silica–Hafnia Thin Film. *J. of Non-crystalline solids*. 401 32-35.

[25] R. G. Hunsperger. (2009). Integrated Optics Theory and Technology, *Sixth Edition. Springer, Chapter 1. ISBN* 978-0-387-89776-9.

[26] N. Kitamura, K. Fukumi, N. Ohno, J. Nishii. (2009). Effect of Hydroxyl Impurity on Temperature Coefficient of Refractive Index of Synthetic Silica Glasses. *J of Non-Cryst. Solids*. 355 2216-2219.

[27] J. M. Nedelec, B. Capoen, S. Turrell, M. Bouazaoui. (2001). Densification and Planar waveguides Doped with rare-earth ions. *J Thin Solid Films*. 382 81-85.

[28] P. Gonzâlez, J. Serra, S. Liste, S. Chiuss, B. LeÓn, M. P. Amor. (2003). Raman Spectroscopic Study of Bioactive Silica Based Glasses. J. Non Cryst. Solids. J of Non-Cryst. Solids. 320 92–99.

[29] L. T. Zhuravlev. (2000). The Surface Chemistry of Amorphous Silica. Zhuravlev Model, Colloids and Surfaces. *J. of A: Physicochemical and Engineering Aspects.* 173 1-38.

[30] D. Carta, M. David. Pickup, J. C. Knowles, I. Ahmed, M. E. Smith, J. R. Newport. (2007). A Structural Study of Sol–Gel and Melt-Quenched Phosphate-Based Glasses. *J. of Non-Crystalline Solids.* 353 1759-1765.

[31] G. C. Righini, S. Pelli, M. Ferrari, C. Armellini, L. Zampedri, C. Tosello, S. Ronchin, R. Rolli, E. Moser, M. Montagna, A. Chiasera, S. J. L. Ribeiro. (2002). Er-Doped Silica-Based Waveguides Prepared by Different Techniques: RF-Sputtering, Sol-Gel and Ion-Exchange. *J Opt. Quant. Electron.* 34 1151.

[32] L. N. Sun, H. J. Zhang, L. S. Fu, F. Y. Liu, Q. G. Meng, C. Y. Peng, J. B. Yu. (2005). A New Sol–Gel Material Doped with an Erbium Complex and Its Potential Optical-Amplification Application, Adv. Funct. Mater. 15 1041–1048.

[33] C. Duverger, M. Montagna, R. Rolly, S. Ronchin, L. Zampedri, M. Fossi, S. Pelli, G. C. Righini, A. Monteil, C. Armellini, M. Ferrari. (2001). Erbium Activated Silica Xerogel: Spectroscopic and Optical Properties. *J. of Non - Cryst. Solids.* 280 261-268.